## Graphical Abstract

To create your abstract, type over the instructions in the template box below.
Fonts or abstract dimensions should not be changed or altered.

**Investigation into the influence of an acrylic acid acceptor in organic D-π-A sensitizers against phototoxicity**

Leave this area blank for abstract info.

Shinichiro Fuse,* Wataru Moriya, Shinichi Sato, and Hiroyuki Nakamura*

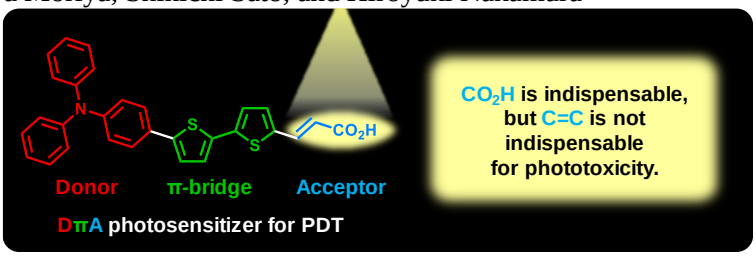

Bioorganic & Medicinal Chemistry
journal homepage: www.elsevier.com

# Investigation into the influence of an acrylic acid acceptor in organic D-π-A sensitizers against phototoxicity

Shinichiro Fuse,[a,*] Wataru Moriya,[b,c] Shinichi Sato,[b] Hiroyuki Nakamura[b,*]

[a] *Department of Basic Medicinal Sciences, Graduate School of Pharmaceutical Sciences, Nagoya University, Furo-cho, Chikusa-ku, Nagoya 464-8601, Japan.*
[b] *Laboratory for Chemistry and Life Science, Institute of Innovative Research, Tokyo Institute of Technology, 4259 Nagatsuta-cho, Midori-ku, Yokohama 226-8503, Japan.*
[c] *School of Life Science and Technology, Tokyo Institute of Technology, 4259 Nagatsuta-cho, Midori-ku, Yokohama 226-8503, Japan.*

ARTICLE INFO

*Article history:*
Received
Received in revised form
Accepted
Available online

*Keywords:*
Photodynamic therapy
Organic dye
Sensitizer
Singlet oxygen
Endocytosis

ABSTRACT

Photodynamic therapy (PDT) is a non-invasive, selective, and cost-effective cancer therapy. We previously reported that thiophene-based organic D-π-A sensitizers consist of an electron-donating (D) moiety, a π-conjugated bridge (π) moiety, and an electron-accepting (A) moiety, and are readily accessible and stable templates for photosensitizers that could be used in PDT. In addition, acrylic acid acceptor-containing photosensitizers exert a high level of phototoxicity. This study was an investigation into 1) the possibility of increasing phototoxicity by introducing another carboxyl group or by replacing a carboxyl group with a pyridinium group, and 2) the importance of an alkene in the acrylic acid acceptor for phototoxicity. A review of the design, synthesis, and evaluation of sensitizers revealed that neither dicarboxylic acid nor pyridinium photosensitizers enhance phototoxicity. An evaluation of a photosensitizer without an alkene in the acrylic acid moiety revealed that the alkene was not indispensable in the pursuit of phototoxicity. The obtained results provided new insight into the design of ideal D-π-A photosensitizers for PDT.

## 1. Introduction

Photodynamic therapy (PDT) is a non-invasive, selective, and cost-effective cancer therapy.[1-8] In PDT, a sensitizer administered to cancer patients damages cancer cells under photo irradiation via Type I (hydrogen/electron transfer) and/or Type II (singlet oxygen generation) pathways, which leads to cell death. There are many requirements for PDT sensitizers: proper absorption wavelength, high absorptivity, high stability under photo irradiation and physiological conditions, low levels of dark toxicity, high levels of tumor accumulation, and rapid excretion from the body following PDT.[9] Tremendous effort has been made to develop new porphyrin-based sensitizers,[9, 10] and several porphyrin-based sensitizers have been approved and clinically used for PDT.[8] Nevertheless, the development of readily accessible and stable templates that allow rapid structural modification for further improvement of PDT remains an important pursuit.

We recently reported the usefulness of thiophene-based organic dyes that combine an electron-donating moiety (D), a π-conjugated bridge moiety (π), and an electron-accepting moiety (A) as readily accessible[11-18] and stable templates for a photosensitizer that could be used in PDT.[19-21] Our previous report revealed the importance of an acrylic acid acceptor for high phototoxicity. Sensitizers **1** and **2**[19] contained an acrylic acid moiety that exerted high levels of phototoxicity, whereas

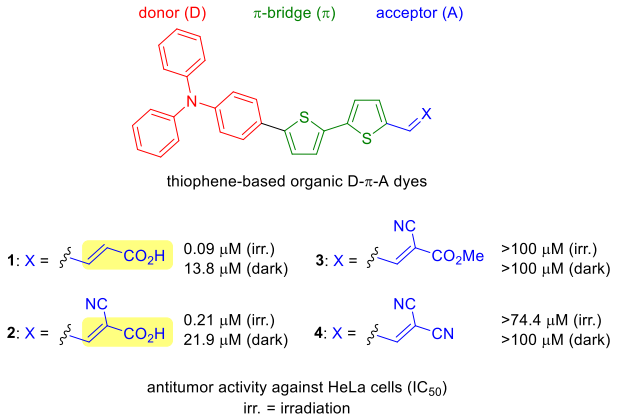


**Fig 1**. Chemical structures and cytotoxic effect of D-π-A sensitizers **1**-**4** with different A moieties. The acrylic acid moiety is highlighted in yellow.

∗ Corresponding author. Tel.: +81-52-747-6927; fax: +81-52-747-6927; e-mail: fuse@ps.nagoya-u.ac.jp

∗ Corresponding author. Tel.: +81-45-924-5244; fax: +81-45-924-5976; e-mail: hiro@res.titech.ac.jp

sensitizers **3**[21] and **4**[19] that contained cyanoacrylate or malononitrile acceptors showed no, or low, levels of phototoxicity. These results showed the importance of carboxyl groups in an acrylic acid acceptor if a high level of phototoxicity is to be achieved. Two questions seemed foremost in this pursuit. 1) Is phototoxicity increased by introducing another carboxyl group or by replacing the carboxyl group with another ionic acceptor? 2) Is a carbon-carbon double bond in the acrylic acid acceptor important for phototoxicity? These basic questions are important for insight into the design of an ideal D-π-A photosensitizer for use in PDT. To address these questions, we describe the design and synthesis of D-π-A sensitizers with a modified acceptor moiety, and report our evaluation of their photophysical, cellular uptake, and photo-oxidizing properties as well as their phototoxicity against HeLa cells.

## 2. Results and Discussion

### *2.1. Design and synthesis of photosensitizers*

Dicarboxylic acid **5** was designed to enhance phototoxicity by increasing the number of carboxyl groups. Pyridinium **6** also was designed to enhance phototoxicity by replacing ionic carboxyl group[22] with another ionic pyridinium group that is known as a good building block for photosensitizers.[23] Carboxylic acids **7** and **8** do not contain a double bond and were designed to examine its importance for phototoxicity (Scheme 1). In accordance with our previously reported procedure,[13, 19] aldehyde **13** was synthesized via a one-pot three-component Suzuki-Miyaura coupling of dibromothiophene **9** with aryl boronic acids **10** and **12**. Knoevenagel condensation of **13** with malonic acid (**14**) and decarboxylation afforded **1**.[19] Hydrogenolysis of the acrylic acid **1** afforded the desired

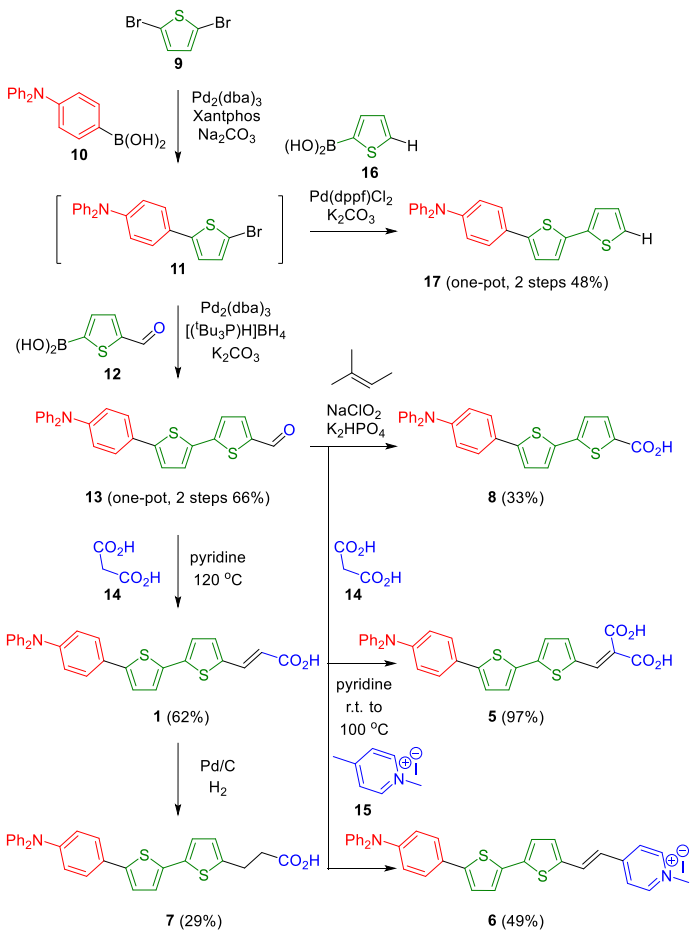


**Scheme 1**. Synthesis of sensitizers that contained a modified acceptor moiety.

carboxylic acid **7**. Pinnick oxidation of the aldehyde **13** afforded the desired carboxylic acid **8**. Dicarboxylic acid **5** was synthesized by Knoevenagel condensation of **13** with **14** under milder conditions that suppressed decarboxylation. The pyridinium **6** was synthesized by Knoevenagel condensation of **13** with pyridinium salts **15**. The sensitizer **17**[11] without an acceptor moiety was also synthesized as a negative control via the one-pot three-component Suzuki-Miyaura coupling of dibromothiophene **9** with aryl boronic acids **10** and **16**. Photosensitizers **5-8** and **1** and **17** (positive and negative controls) were prepared for use in the following evaluations.

### *2.2. Photoabsorptive and fluorescence properties of sensitizers*

The absorption spectra of sensitizers are shown in Figure 2 and Table 1. The photoabsorptivity of sensitizers **5-7** was slightly decreased compared with that of **1**, while that of **8** and **17** was significantly decreased. The spacer (CH=CH or $CH_2$-$CH_2$) between thiophene ring and carboxyl or pyridinium group might be important for high photoabsorptivity. The absorption maxima of sensitizer **6** contained a strong electron-withdrawing pyridinium acceptor was red-shifted compared with that of sensitizer **1**. The absorption maxima of dicarboxylic acid **5** was not changed from that of sensitizer **1**, although **5** has an additional electron-withdrawing carboxyl acceptor. This was probably due to the deprotonation of the carboxylic acid in the PBS buffer, as it decreased the electron-withdrawing ability of carboxylic acid and raised the LUMO level of **5**. We previously observed a dramatic change in the absorption wavelength of the

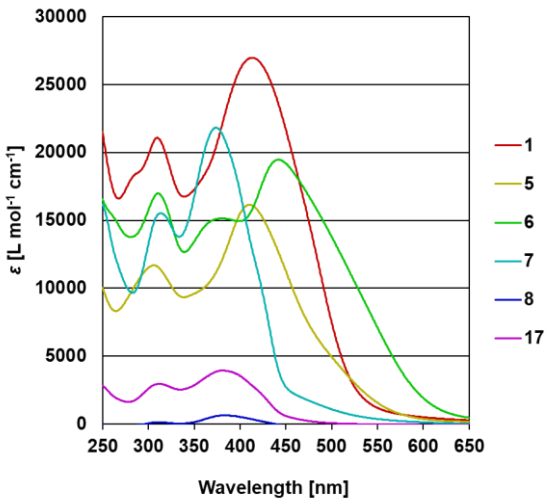


**Fig 2**. Absorption spectra of D-π-A sensitizers (50 μM) in deionized water.

**Table 1.** The photoabsorptive properties of D-π-A sensitizers.

| sensitizer | $\varepsilon$ [L mol$^{-1}$ cm$^{-1}$][a] | $\lambda_{max}$ [nm][b] | optical edge [nm][c] |
|---|---|---|---|
| **1** | $2.69 \times 10^4$ | 414 | 525 |
| **5** | $1.62 \times 10^4$ | 410 | 549 |
| **6** | $1.95 \times 10^4$ | 442 | 600 |
| **7** | $2.18 \times 10^4$ | 374 | 460 |
| **8** | $6.49 \times 10^2$ | 383 | 435 |
| **17** | $3.94 \times 10^3$ | 382 | 463 |

[a] Molar absorption coefficients.

[b] Absorption maxima.

[c] Optical absorption edge was defined by the wavelength for which the absorbance revealed 1/10 of peak top.

carboxyl acceptor-containing sensitizer by changing the pH [20]. The absorption maxima of sensitizers **7** and **17** were blue-shifted compared with that of **1**. Unexpectedly, the absorption maxima of sensitizer **8** was also blue-shifted. This is also probably due to the deprotonation of the carboxyl acceptor in **8**.

Essentially, fluorescence is not desirable for photosensitizers in PDT, because they lose excitation energy by emitting fluorescence that leads to a decrease in photo-oxidizing ability. Evaluation of the fluorescence properties of the sensitizers revealed that their fluorescence emissions were too weak to impair their photo-oxidizing abilities (for details, see supporting information Table S1). Interestingly, the sensitizers **8** and **17** without the spacer that showed very low photoabsorptivity exerted relatively high intensity of fluorescence emissions compared with those of other sensitizers.

### *2.3. Photo-oxidizing ability of the sensitizers*

The photo-oxidizing ability of the sensitizers was evaluated using human serum albumin (HSA). HSA has only one tryptophan residue, from which almost the entire amount of intrinsic fluorescence of HSA originates. Photo-irradiated sensitizers easily oxidize this tryptophan residue, which results in a decrease in its characteristic fluorescence at around 350 nm. Therefore, HSA is useful for evaluating the protein-damaging activity of photosensitizers.[24-28] A sample solution containing 10 μM of a photosensitizer and 20 μM of HSA in a PBS buffer was irradiated via LED lighting (white LED, ISL-150×150 H3WH4R, 420-750 nm, 8.0±0.5 mW/cm$^2$, CCS Inc. Figure S1). The highest oxidative damage of HSA was observed in the case of dicarboxylic acid **5** (Figure 3a). Pyridinium **6** also exerted a high level of HSA damage. Photosensitizers **7**, **8**, and **17**, each of which contains no alkene moiety, showed similar, and moderate, levels of oxidative damage compared with that of **1**. These results indicated that the alkene in the acrylic acid acceptor is not indispensable in order to accomplish photo-oxidization.

HSA is known to be a main carrier of fatty acids,[29] which means it is possible that carboxylic acid-containing compounds **1**, **5**, **7**, and **8** could bind to HSA. Therefore, we were concerned that if these compounds, particularly dicarboxylic acid **5**, strongly

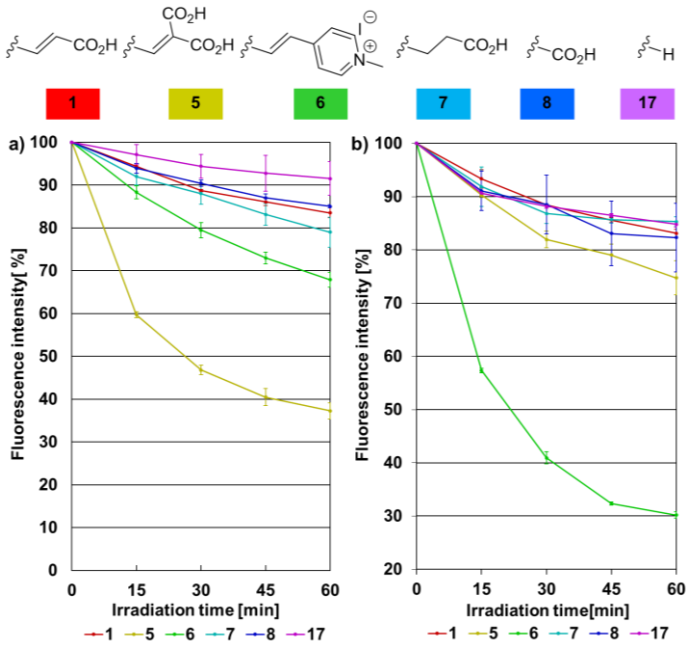


**Fig 3**. Time-dependent damage to HSA (a) and to H-Trp-OH (b) that is caused by the photo-irradiation of sensitizers.

interacted with HSA. It could lead to an overestimation of their photo-oxidizing abilities. Therefore, the photo-oxidizing ability of the photosensitizers was also evaluated using L-tryptophan (H-Trp-OH). A sample solution containing 10 μM of photosensitizer and 20 μM of H-Trp-OH in a PBS buffer was irradiated via LED lighting (Figure 3b). Although the tryptophan residue in HSA is buried in the protein structure, H-Trp-OH is not hindered and is more likely to be oxidized. In the case of dicarboxylic acid **5**, however, the oxidative damage to H-Trp-OH was significantly decreased compared with that to HSA. We speculated that a strong interaction between dicarboxylic acid and HSA induced a faster rate of the damage to HSA. The level of oxidative damage to H-Trp-OH was similar to that of HSA in the cases of photosensitizers **1**, **7**, **8**, and **17**. A significantly higher level of oxidative damage to H-Trp-OH was observed in the case of pyridinium **6**, which was probably due to the absence of steric hindrance from the protein. A similar level of oxidative damage to H-Trp-OMe was observed in the case of **6** (Figure S2). These results indicate that special care should be taken when using HSA to evaluate the photo-oxidation ability of photosensitizers, when the photosensitizers have particular interactions with HSA.

To further elucidate the mode of action, we monitored the damage to human serum albumin (HSA) caused by the photo irradiation of sensitizers **5** and **6** in the presence of different additives ($NaN_3$ or D-mannitol) caused by the photo-irradiation of sensitizers **5** and **6**. The addition of D-mannitol (Type I hydroxyl radical quencher) slightly decreased the damage to HSA in the case of sensitizer **6**, although it was not a significant level (Figure S3). The type I mechanism that was inhibited by D-mannitol might be important for the photo-oxidizing ability of **6**. The addition of $NaN_3$ (Type II singlet oxygen quencher) significantly decreased the damage to HSA and H-Trp-OH in the case of sensitizer **5** (Figure S3). These results indicated that Type II is a major mechanism in the photo-oxidizing ability of sensitizer **5**.

### *2.4. Cellular uptake study*

The cellular uptake of photosensitizers was investigated (Figure 4). In order to examine the contribution of endocytosis[30, 31] to the cellular uptake of photosensitizers, they were incubated with HeLa cells either at 37 °C under normal conditions or at 4 °C under conditions that suppress energy-dependent vesicular transport. Endocytosis is an energy-dependent mechanism, and, therefore, it is suppressed at 4 °C. Following incubation, the medium was removed, and the cells were washed and lysed with DMSO. The amount of photosensitizers was determined by measuring their fluorescence intensity using a calibration curve. The amounts of acrylic acid **1**, dicarboxylic acid **5**, and thiophene **17** were similar, and the contribution from endocytosis was relatively lower than that for other photosensitizers. On the contrary, the amount of photosensitizers **6**-**8** was obviously higher than that of other photosensitizers. The contribution from endocytosis was significant in the cases of **7** and **8**. These results indicated that the alkene in the acrylic acid acceptor was not indispensable for the cellular uptake of photosensitizers. The number of photosensitizers was highest in the case of **6**. We speculated that the cationic photosensitizer **6** strongly interacts with the anionic phospholipids in the cellular membrane and this resulted in the high level of cellular uptake that was observed.

Because photosensitizers **6**-**8** showed significant endocytosis-mediated cellular uptake, the mechanism of endocytosis was investigated. HeLa cells were incubated with the photosensitizers at 37 °C in the presence/absence of sucrose, methyl-β-cyclodextrin (MβCD), and wortmannin, which are inhibitors of

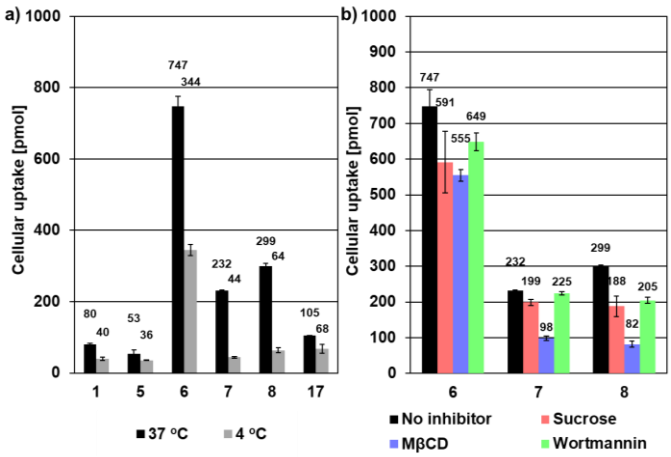


**Fig 4**. Cellular uptake of photosensitizers by HeLa cells at 37 and 4 °C (a); cellular uptake of photosensitizers **6**-**8** without/with inhibitors (b).

clathrin-mediated endocytosis,[32] lipid raft endocytosis, and endosome fusion,[33] respectively. Following incubation, the medium was removed, the cells were washed and lysed, and the photosensitizer amounts were determined (Figure 4b). None of the three inhibitors significantly suppressed the cellular uptake of pyridinium **6**. Other mechanisms could play important roles in the cellular uptake of **6**. The other hand, MβCD obviously suppressed the cellular uptake of carboxylic acids **7** and **8**. This indicated that lipid raft endocytosis played an important role in the cellular uptake of photosensitizers **7** and **8**. This tendency is consistent with that of photosensitizer **1**, which contains a cyanoacrylic acid acceptor.[21] D-π-A photosensitizers containing a carboxyl group might preferentially move into cells via lipid raft endocytosis.

We also performed dynamic light scattering (DLS) measurement in order to confirm the formation of aggregates by photosensitizers in PBS buffer. As a result, aggregate formation was observed (for details, see supporting information Figure S4). However, no clear relationship was observed between the particle size and cellular uptake.

*2.5. Colocalization study*

In order to confirm the cellular uptake and localization of the photosensitizers, HeLa cells were treated with photosensitizers and commercially available fluorescent probes for mitochondria and lysosome, and were observed using fluorescence confocal microscopy (for details, see supporting information Figures S5, S6, and Table S2). Mitochondria and lysosomes are targets of many reported photosensitizers,[34] and obvious fluorescence was detected at the mitochondria and lysosomes in all the cases of photosensitizers. In addition, the localization of pyridinium **6** was observed at the cellular membrane (Figure S6). This observation corroborated our previous speculation that pyridinium **6** tended to interact with anionic phospholipids in the cellular membrane.

*2.6. Phototoxicity of the sensitizers*

The antitumor effects of photosensitizers on HeLa cells under photo irradiation are shown in Table 2. Dicarboxylic acid **5** and pyridinium **6** showed a slightly lower level of photoabsorption, a higher level of photo-oxidizing ability, and a similar or higher level of cellular uptake compared with that of **1**. Unexpectedly, however, their phototoxic index (PI) was lower than **1**. Although the reasons are unclear, strong interactions of **5** and **6** with albumin and the cellular membrane could have a negative impact on their phototoxicity. In addition, a relatively high level of dark

**Table 2.** Antitumor activity of the photosensitizers against HeLa cells.

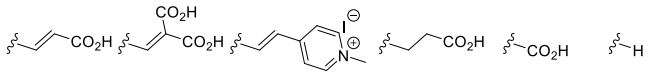


| photosensitizer | $IC_{50}$ (μM)[a] | | PI[b] |
|---|---|---|---|
| | dark | irradiation | |
| **1** | 20.9 ± 4.5 | 0.046 ± 0.012 | 460 |
| **5** | 61.8 ± 6.5 | 0.68 ± 0.05 | 91 |
| **6** | 3.3 ± 0.3 | 0.94 ± 0.03 | 3.5 |
| **7** | 43.4 ± 1.0 | 2.4 ± 0.1 | 18 |
| **8** | >100 | 7.8 ± 1.5 | >12 |
| **17** | >100 | >100 | - |

[a] The photosensitizer concentration required to reduce cell viability by 50% ($IC_{50}$) was determined from semi-logarithmic, dose-response plots.
[b] PI = phototoxicity index; PI is the ratio of the $IC_{50}$ values in the dark to those obtained upon light irradiation.

toxicity was observed for pyridinium **6**, which is attributable to a strong interaction between cationic pyridinium **6** and a negative phospholipid that leads to membrane disruption. Negative control of photosensitizer **17** showed no cytotoxicity under either dark or irradiation conditions ($IC_{50}$ >100 μM). On the other hand, carboxylic acids **5** and **6** showed obvious phototoxicity ($IC_{50}$ = 2.4 and 7.8 μM, respectively), although their photoabsorption was very poor due to the mismatch between their absorption wavelength (Figure 2) and the emission wavelength of LED light (420-750 nm). These results indicated that the alkene in the acrylic acid acceptor is not indispensable for phototoxicity. Therefore, again we confirmed the importance of carboxylic acid to the high phototoxicity of D-π-A photosensitizers.

## 3. Conclusions

This investigation had two major objectives: 1) the possibility of increasing phototoxicity either by introducing another carboxyl group or by replacing carboxyl groups with pyridinium groups; and, 2) determining the importance of alkene in the acrylic acid acceptors of D-π-A photosensitizers for phototoxicity. Although dicarboxylic acid **5** and pyridinium **6** exerted higher levels of photo-oxidizing ability and similar, or higher, levels of cellular uptake compared with those of **1**, their PI was unexpectedly lower than that of **1**. The evaluation of photo-oxidizing and cellular uptake properties as well as phototoxicity revealed that alkene was not indispensable, although it demonstrated a positive influence on the photophysical properties. These results suggest new design guidelines for D-π-A photosensitizers. Strong electron-withdrawing acceptors should be directly connected to π-conjugation systems rather than a mildly electron-withdrawing carboxyl group (the electron-withdrawing ability of carboxylic acid is further decreased by deprotonation) in order to realize near IR absorption. In addition, one carboxylic acid should be connected to the photosensitizer in order to enhance its phototoxicity. The design and synthesis of new synthesizers based on the design guidelines discussed here is ongoing by our group.

## 4. Experimental section

*4.1. General methods*

NMR spectra were recorded on either a BRUKER BIOSPIN AVANCE II 400 (400 MHz for $^{1}H$, 100 MHz for $^{13}C$) or a BRUKER BIOSPIN AVANCE III HD500 (500 MHz for $^{1}H$, 125

MHz for $^{13}C$) in the indicated solvent. Chemical shifts are reported in units of parts per million (ppm) relative to tetramethylsilane (0.00 ppm) or $CDCl_3$ (7.26 ppm) or DMSO-$d_6$ (2.50 ppm) for $^1H$ NMR and $CDCl_3$ (77.2 ppm) or DMSO-$d_6$ (39.5 ppm) for $^{13}C$ NMR. Multiplicities are reported using the following abbreviations: s, singlet; d, doublet; dd, doublet of doublets; t, triplet; m, multiplet; and *J*, coupling constants in Herts (Hz). Particle sizes were measured using an electrophoretic light scattering spectrophotometer. IR spectra were recorded on a JASCO Corporation FT/IR-4100 FT-IR Spectrometer. An ATR PRO ONE was attached to the FT/IR-4100 to measure solid IR spectroscopy via single reflection attenuated total reflection. Only the strongest and/or structurally important peaks were reported as the IR data given in $cm^{-1}$. The absorption spectra were measured with JASCO V-670. HRMS (ESI-TOF-MS) were measured using a Bruker micrOTOF II. All reactions were monitored by thin layer chromatography carried out on 0.2 mm E. Merck silica gel plates (60 $F_{254}$) with UV light, visualized by *p*-anisaldehyde solution or 10% ethanolic phosphomolybdic acid. Flash column chromatography was performed on silica gel (Fuji Silysia, CHROMATOREX PSQ 60B, 50-200 μm). Gel permeation chromatography (GPC) purification was performed on a Japan Analytical Industry Model LC-9225NEXT (recycling preparative HPLC) using a UV detector and a polystyrene gel column (JAIGEL-1H, 20 nm×600 mm) with $CHCl_3$ as a solvent (3.5 mL/min). A photo of the white LED light source (ISL-150×150 H3WH4R, 8.0±0.5 mW/cm$^2$, CCS Inc.) is shown in Figure S1. This light source was equipped with 180 small white LED lamps and 180 small red LED lamps, and, thus, it allowed both white and red light irradiation. However, only the white LED light irradiation {$\lambda_{max}$ = 460 nm (relative irradiance: 100%), 560 nm (relative irradiance: 40%); $\lambda$ = 420-750 nm} was used for our research.

*4.2. 5'-(4-(Diphenylamino)phenyl)(2,2'-bithiophene)-5-carboxaldehyde (**13**).[13, 19]*

A solution of boronic acid **10** (509 mg, 1.76 mmol, 1.10 eq.), 2,5-dibromothiophene (**9**) (0.180 mL, 1.60 mmol, 1.00 eq.), Xantphos (18.5 mg, 0.0320 mmol, 0.0200 eq.), $Na_2CO_3$ (339 mg, 3.20 mmol, 2.00 eq.), $Pd_2(dba)_3$ (14.7 mg, 0.0160 mmol, 0.0100 eq.) in THF (8.00 mL), and $H_2O$ (8.00 mL) was degassed with Ar. After stirring the mixture at reflux temperature (80 °C) for 4 h, boronic acid **12** (349 mg, 2.24 mmol, 1.40 eq.), [($^tBu_3P$)H]$BF_4$ (23.2 mg, 0.0800 mmol, 0.0500 eq.), $Na_2CO_3$ (339 mg, 3.20 mmol, 2.00 eq.), and $Pd_2(dba)_3$ (19.2 mg, 0.021 mmol, 0.0300 eq.) were added to the mixture. After being stirred at room temperature for 4 h, the reaction mixture was passed through a pad of Celite®, poured into $H_2O$, and extracted with $CH_2Cl_2$/toluene. The extract was dried over $MgSO_4$, filtered and concentrated in vacuo. The residue was purified by column chromatography on silica gel eluted with 50 to 80% $CH_2Cl_2$ in hexane, to afford **13** as orange solids. Yield (one-pot two steps): 68% (598 mg, 1.37 mmol). $^1H$ NMR (400 MHz, $CDCl_3$): δ 9.85 (s, 1H), 7.67 (d, *J* = 3.9 Hz, 1H), 7.46 (d, *J* = 8.7 Hz, 2H), 7.32 (d, *J* = 3.9 Hz, 1H), 7.30-7.28 (m, 4H), 7.24 (d, *J* = 3.9 Hz, 1H), 7.17 (d, *J* = 3.9 Hz, 1H), 7.13 (d, *J* = 8.7 Hz, 4H), 7.10-7.03 (m, 4H). The observed $^1H$ NMR spectrum was consistent with the reported NMR spectrum.[13, 19]

*4.3. 2-((5'-(4-(Diphenylamino)phenyl)-(2,2'-bithiophen)-5-yl)methylene)malonic acid (**5**).*

To a solution of aldehyde **13** (80.0 mg, 0.180 mmol, 1.00 eq.) and malonic acid (93.7 mg, 0.900 mmol, 5.00 eq.) in pyridine (1.80 mL), piperidine (0.0286 mL, 0.0290 mmol, 1.60 eq.) was added dropwise at 0 °C under Ar. After being stirred at the same temperature for 1 h, the resultant mixture was heated at 100 °C with stirring for 2 h. The reaction mixture was poured into $H_2O$, and extracted with $CH_2Cl_2$. The extract was dried over $MgSO_4$, filtered and concentrated in vacuo. The residue was purified by column chromatography on silica gel eluted with 9% MeOH in $CH_2Cl_2$, to afford **5** as red solids. Yield: 94% (80.1 mg, 0.168 mmol). Mp: 148-150 °C; $^1H$ NMR (400 MHz, DMSO-$d_6$): δ 8.03 (s, 1H), 7.61-7.55 (m, 3H), 7.44-7.40 (m, 2H), 7.36 (d, *J* = 3.8 Hz, 1H), 7.32 (t, 4H), 7.12-7.01 (m, 6H), 6.96 (d, *J* = 8.8 Hz, 2H); $^{13}C$ NMR (125 MHz, DMSO-$d_6$): δ 168.8, 168.3, 147.3, 146.8, 144.3, 143.6, 139.5, 137.0, 135.8, 134.6, 129.8, 127.0, 126.6, 126.5, 124.5, 124.1, 123.7, 123.4, 122.8, 120.0; HRMS (ESI-TOF): calcd. for $C_{30}H_{21}NO_4S_2$ $[M-H]^-$ 522.0834, found 522.0776.

*4.4. (E)-4-(2-(5'-(4-(Diphenylamino)phenyl)-(2,2'-bithiophen)-5-yl)vinyl)-1-methylpyridin-1-ium iodide (**6**).*

To a solution of aldehyde **13** (50.0 mg, 0.114 mmol, 1.00 eq.) and 1,4-dimethylpyridin-1-ium iodide **15** (29.0 mg, 0.125 mmol, 1.10 eq.) in toluene (1.1 mL), piperidine (11 μL, 0.11 mmol, 1.0 eq.) was added dropwise at room temperature. After being stirred at reflux temperature (120 °C) for 6 h, the reaction mixture was cooled to room temperature and poured into $H_2O$, extracted with $CH_2Cl_2$ and ethyl acetate, dried over anhydrous $Na_2SO_4$, and filtered and concentrated in vacuo. The residue was purified by chromatography on silica gel eluted with 10% MeOH in $CH_2Cl_2$, and target compound **6** was obtained as dark magenta solids. Yield: 49% (36.3 mg, 0.0555 mmol). Mp: 256-261 °C; $^1H$ NMR (500 MHz, DMSO-$d_6$): δ 8.78 (d, *J* = 6.8 Hz, 2H), 8.18 (d, *J* =16.1 Hz, 1H), 8.14 (d, *J* = 7.0 Hz, 2H), 7.60 (d, *J* = 8.7 Hz, 2H), 7.49-7.42 (m, 4H), 7.34 (t, *J* = 8.1 Hz, 4H), 7.14 (d, *J* = 16.0, 1H), 7.10 (t, *J* = 7.0 Hz, 2H), 7.07 (d, *J* = 8.7 Hz, 4H), 6.98 (d, *J* = 8.6 Hz, 2H), 4.21 (s, 3H); $^{13}C$ NMR (125 MHz, DMSO-$d_6$): δ 152.5, 147.8, 147.2, 145.3, 144.3, 140.5, 139.4, 134.4, 134.0, 133.8, 134.4, 130.2, 127.3, 127.1, 127.0, 125.6, 125.0, 124.6, 124.2, 123.2, 122.2, 47.3; HRMS (ESI-TOF): calcd. for $C_{34}H_{27}N_2S_2$ $[M]^+$ 527.1610, found 527.1610.

*4.5. 5'-(4-(Diphenylamino)phenyl)-(2,2'-bithiophene)-5-carboxylic acid (**8**).*

A solution of aldehyde **13** (81.0 mg, 0.19 mmol, 1.0 eq.), 2-methyl-2-butene (0.99 mL, 9.5 mmol, 50 eq.), 330 mg of $K_2HPO_4$ (330 mg, 1.89 mmol, 1.00 eq.) and $NaClO_2$ (170 mg, 1.89 mmol, 1.00 eq.) in THF (2.0 mL), $^tBuOH$ (0.57 mL), and $H_2O$ (3 drops) was stirred at room temperature for 4 h. Then, 1.0 M HCl aq. (3.0 mL) was added to the mixture at the same temperature. The resultant reaction mixture was poured into $H_2O$, extracted with $CH_2Cl_2$, dried over $Na_2SO_4$ and concentrated in vacuo. The residue was purified by column chromatography on silica gel eluted with 40 to 50% EtOAc in toluene, and further purified by GPC to afford **2-3** as yellow solid. Yield: 29% (25.0 mg, 0.0550 mmol). Mp: 239-241 °C; $^1H$ NMR (400 MHz, $CDCl_3$) δ 7.64 (d, *J* = 4.0 Hz, 1H), 7.46 (d, *J* = 8.6 Hz, 2H), 7.31-7.26 (m, 5H), 7.18-7.15 (m, 2H) 7.13 (d, *J* = 8.5 Hz, 4H), 7.07 (d, *J* = 8.2 Hz, 2H), 7.05 (t, *J* = 7.1 Hz, 2H); $^{13}C$ NMR (125 MHz, DMSO-$d_6$) δ 163.2, 147.7, 147.1, 144.4, 143.2, 134.7, 134.1, 132.9, 130.1, 127.5, 127.1, 127.0, 124.9, 124.8, 124.4, 124.1, 123.1; HRMS (ESI-TOF): calcd. for $C_{27}H_{19}NO_2S_2$ $[M-H]^-$ 452.0779, found 452.0638.

*4.6. (E)-3-(5'-(4-(Diphenylamino)phenyl)-(2,2'-bithiophen)-5-yl)acrylic acid (**1**).*[19]

To a solution of aldehyde **13** (50.0 mg, 0.114 mmol, 1.00 eq.) and malonic acid (60.0 mg, 0.562 mmol, 5.00 eq.) in pyridine (1 mL), piperidine (18 μL, 0.18 mmol, 1.6 equiv.) was added dropwise at 0 °C under Ar. The solution then was immediately heated to 120 °C and stirred for 3 h. The reaction mixture was cooled and poured into $H_2O$, and extracted with $CH_2Cl_2$. The extract was dried over $MgSO_4$, filtered and concentrated in vacuo. The residue was purified by column chromatography eluted with 9% MeOH in $CH_2Cl_2$ to afford **1** as orange solids. Yield:

61% (33.0 mg, 0.0690 mmol). $^1$H NMR (500 MHz, DMSO-$d_6$): δ 7.70 (d, $J$ = 15.6 Hz, 1H), 7.59 (d, $J$ = 8.8 Hz, 2H), 7.47 (d, $J$ = 3.9 Hz, 1H), 7.42 (m, 2H), 7.35-7.32 (m, 5H), 7.11-7.06 (m, 6H), 6.98 (d, $J$ = 8.8 Hz, 2H), 6.13 (d, $J$ = 15.6 Hz, 1H). The observed $^1$H NMR spectrum was consistent with the reported NMR spectra.[19]

*4.7. 3-(5'-(4-(Diphenylamino)phenyl)-(2,2'-bithiophen)-5-yl)propanoic acid (**7**).*

To a solution of acrylic acid **1** (62.0 mg, 0.129 mmol, 1.00 eq.) in 1.2 mL of THF was added palladium 10% on carbon (13.8 mg, 0.0129 mmol, 0.100 eq.). After filling with argon, argon gas replaced the hydrogen gas. After being stirred at room temperature for 11 h, the palladium was inactivated by the introduction of argon, passed through Celite®, and concentrated in vacuo. The residue was purified by column chromatography on silica gel eluted with 9% MeOH in $CH_2Cl_2$, and further purified by preparative TLC to afford **7** as brown solid. Yield: 29% (18.0 mg, 0.0380 mmol). Mp: 142-144 °C; $^1$H NMR (400 MHz, $CDCl_3$ and 20% MeOD): δ 7.44 (d, $J$ = 8.6, 2H), 7.29-7.24 (m, 6H), 7.14-7.08 (m, 4H), 7.07-7.03 (m, 4H), 6.98 (d, $J$ = 3.4 Hz, 1H), 6.75 (d, $J$ = 3.4 Hz, 1H), 3.15 (t, $J$ = 7.3 Hz, 2H), 2.74 (t, $J$ = 7.3 Hz, 2H); $^{13}$C NMR (125 MHz, $CDCl_3$ and 20% MeOD): δ 147.6, 147.3, 142.8, 141.8, 135.9, 135.9, 129.3, 128.1, 126.3, 125.6, 124.5, 124.2, 123.6, 123.2, 123.1, 122.8, 35.6, 29.7, 25.1; HRMS (ESI-TOF): calcd. for $C_{29}H_{23}NO_2S_2$ $[M-H]^-$ 480.1092, found 480.0987.

*4.8. 4-((2,2'-Bithiophen)-5-yl)-N,N-diphenylaniline (**17**).*

A solution of boronic acid **10** (400 mg, 1.38 mmol, 1.10 eq.), 2,5-dibromothiophene (**9**) (0.142 mL, 1.26 mmol, 1.00 eq.), Xantphos (11.6 mg, 12.6 μmol, 0.0200 eq.), $Pd_2(dba)_3$ (9.2 mg, 25 μmol, 0.010 eq.), and $Na_2CO_3$ (267 mg, 2.52 mmol, 2.00 eq.) in THF (6.3 mL) and $H_2O$ (6.3 mL) was degassed with Ar. After being stirred at reflux temperature (80 °C) for 4 h, thiophen-2-ylboronic acid (**16**) (225 mg, 1.76 mmol, 1.40 eq.), $Na_2CO_3$ (348 mg, 2.52 mmol, 2.00 eq.), and $Pd(dppf)Cl_2$ (36.6 mg, 0.063 mmol, 0.0500 eq.) were added to the mixture. After stirring at 80 °C for 10 h, the reaction mixture was passed through Celite®, and poured into $H_2O$, and extracted with $CH_2Cl_2$/ethyl acetate. The extract was dried over $MgSO_4$, filtered and concentrated in vacuo. The residue was purified by column chromatography on silica gel eluted with 8 to 16% EtOAc in hexane, to afford **17** as yellow solids. Yield (one-pot 2 steps): 48% (250 mg, 0.610 mmol). $^1$H NMR (400 MHz, $CDCl_3$): δ 7.46 (d, $J$ = 8.8 Hz, 2H), 7.30-7.24 (m, 4H), 7.21 (dd, $J$ = 5.3, 1.0 Hz, 1H), 7.18 (dd, $J$ = 3.9 Hz, 1.0 Hz, 1H), 7.14-7.10 (m, 6H), 7.08-7.00 (m, 5H). The observed NMR spectrum was consistent with the reported NMR spectrum.[11]

*4.9. Evaluation of HSA or H-Trp-OH or H-Trp-OMe damage by photosensitizers.*

Sample solutions containing photosensitizer (10 μM) and either HSA, H-Trp-OH, or H-Trp-OMe (20 μM) in PBS buffer were irradiated by white LED (ISL-150×150 H3WH4R, 8.0±0.5 mW/cm$^2$, CCS Inc., Kyoto, Japan) for 15 minutes each, 60 min total. The damage to the HSA, the H-Trp-OH, and the H-Trp-OMe by the photosensitizer was evaluated by measuring the fluorescence intensity at 334 nm ($\lambda_{ex}$ = 298 nm) from the tryptophan residue.

*4.10. Cellular uptake of photosensitizers.*

HeLa cells (5×10$^4$ cells) were plated in 24-well plates and incubated with photosensitizer (20 μM) at 37 °C for 1 h. After the incubation, the medium was removed, washed twice with PBS buffer and solubilized by the addition of lysis buffer (500 μL, 20 mM Tris, 150 mM NaCl, 1 mM EDTA, 1 mM EGTA, 1×TritonX). The amount of subcellular uptake of photosensitizer was determined from the measurement of fluorescence intensity of photosensitizer using calibration curves.

*4.11. Cellular uptake mechanism of photosensitizers.*

HeLa cells (5.0×10$^4$ cells) were plated in 24-well plates and pre-treated with specific endocytosis inhibitor (MβCD or sucrose or wortmannin) for 1 h either at 37 or 4 °C. After removing the inhibitor, the washed PBS and cells were incubated with the photosensitizer (20 μM) at either 37 °C or 4 °C for 1 h. Following incubation, the medium was removed, and the cells were washed twice with PBS and solubilized by the addition of lysis buffer (500 μL, 20 mM Tris, 150 mM NaCl, 1 mM EDTA, 1 mM EGTA, 1×TritonX). The subcellular uptake amount of photosensitizer was determined by measuring the fluorescence intensity of the photosensitizer using calibration curves.

*4.12. Cell viability assay (MTT assay, without light irradiation).*

Human cervical carcinoma HeLa cells were used for the cell viability assay. These cells (5×10$^3$ cells per well of a 96-well plate) were incubated at 37 °C for 48 h in RPMI-1640 medium (100 μL) containing various concentrations of photosensitizers (10 mM DMSO solution). Following incubation, the medium was removed, RPMI-1640 medium (100 μL) and 3'-(4,5-dimethylthiazol-2-yl)-2,5-diphenyltetrazolium bromide (MTT) in PBS (5 mg/mL, 10 μL) were added to each well, and the cells were further incubated at 37 °C for 2 h. After removal of the medium, DMSO (100 μL) was added and the absorbance at 595 nm was measured with a microplate reader. The drug concentration required to reduce cell viability by 50% ($IC_{50}$) was determined from semilogarithmic dose-response plots.

*4.13. Cell viability assay (HeLa cell, MTT assay, with light irradiation).*

Human cervical carcinoma HeLa cells were used for the cell viability assay. These cells (5×10$^3$ cells per well of a 96-well plate) were incubated at 37 °C for 1 h in RPMI-1640 medium (100 μL) containing various concentrations of a photosensitizer (10 mM DMSO solution), and then the cells were irradiated by white LED (ISL-150×150 H3WH4R, 8.0±0.5 mW/cm, CCS Inc.) for 15 min. After incubation for 48 h, the medium was removed, RPMI-1640 medium (100 μL) and MTT in PBS (5 mg/mL, 10 μL) were added to each well, and the cells were further incubated at 37 °C for 2 h. After removal of the medium, DMSO (100 μL) was added and the absorbance at 595 nm was measured with a microplate reader. The drug concentration required to reduce cell viability by 50% ($IC_{50}$) was determined from semilogarithmic dose-response plots.

## Supplementary Material

Supplementary data associated with this article can be found, in the online version, at https://doi.org/10.1016/j.bmc.xxxx.xx.xxx.

## References and notes

[1] Dolmans, D. E. J. G. J.; Fukumura, D., Jain, R. K. Photodynamic therapy for cancer, Nat. Rev. Cancer, 3 (2003) 380-387.
[2] Huang, Z. A review of progress in clinical photodynamic therapy, Technol. Cancer Res. Treat., 4 (2005) 283-293.
[3] Robertson, C. A.; Evans, D. H., Abrahamse, H. Photodynamic therapy (PDT): A short review on cellular mechanisms and cancer research applications for PDT, J. Photochem. Photobiol. B: Biol., 96 (2009) 1-8.

[4] Agostinis, P.; Berg, K.; Cengel, K. A.; Foster, T. H.; Girotti, A. W.; Gollnick, S. O.; Hahn, S. M.; Hamblin, M. R.; Juzeniene, A.; Kessel, D.; Korbelik, M.; Moan, J.; Mroz, P.; Nowis, D.; Piette, J.; Wilson, B. C., Golab, J. Photodynamic therapy of cancer: an update, CA Cancer J. Clin., 61 (2011) 250-281.
[5] Allison, R. R., Moghissi, K. Photodynamic therapy (PDT): PDT mechanisms, Clin Endosc, 46 (2013) 24-29.
[6] Lucky, S. S.; Soo, K. C., Zhang, Y. Nanoparticles in photodynamic therapy, Chem. Rev., 115 (2015) 1990-2042.
[7] Fan, W.; Huang, P., Chen, X. Overcoming the Achilles' heel of photodynamic therapy, Chem. Soc. Rev., 45 (2016) 6488-6519.
[8] dos Santos, A. F.; de Almeida, D. R. Q.; Terra, L. F.; Baptista, M. S., Labriola, L. Photodynamic therapy in cancer treatment - an update review, J. Cancer Metastasis Treat., 5 (2019).
[9] Ormond, A. B., Freeman, H. S. Dye sensitizers for photodynamic therapy, Materials, 6 (2013) 817-840.
[10] Yuan, A.; Wu, J.; Tang, X.; Zhao, L.; Xu, F., Hu, Y. Application of near-infrared dyes for tumor imaging, photothermal, and photodynamic therapies, J. Pharm. Sci., 102 (2013) 6-28.
[11] We previously reported synthesis of **17** via iterative Pd-catalyzed coupling approach. see, Fuse, S.; Yoshida, H., Takahashi, T. An iterative approach to the synthesis of thiophene-based organic dyes, Tetrahedron Lett., 53 (2012) 3288-3291. However, we have not evaluated its ability for photosensitizer of PDT.
[12] Fuse, S.; Asai, Y.; Sugiyama, S.; Matsumura, K.; Maitani, M. M.; Wada, Y.; Ogomi, Y.; Hayase, S.; Kaiho, T., Takahashi, T. Synthesis of EDOT-containing organic dyes via one-pot, four-component Suzuki-Miyaura coupling and the evaluation of their photovoltaic properties, Tetrahedron, 70 (2014) 8690-8695.
[13] Fuse, S.; Matsumura, K.; Fujita, Y.; Sugimoto, H., Takahashi, T. Development of dual targeting inhibitors against aggregations of amyloid-β and tau protein, Eur. J. Med. Chem., 85 (2014) 228-234.
[14] Fuse, S.; Matsumura, K.; Wakamiya, A.; Masui, H.; Tanaka, H.; Yoshikawa, S., Takahashi, T. Elucidation of the structure-property relationship of p-type organic semiconductors through rapid library construction via a one-pot, Suzuki-Miyaura coupling reaction, ACS Comb. Sci., 16 (2014) 494-499.
[15] Fuse, S.; Sugiyama, S.; Maitani, M. M.; Wada, Y.; Ogomi, Y.; Hayase, S.; Katoh, R.; Kaiho, T., Takahashi, T. Elucidating the structure-property relationships of donor-π-acceptor dyes for dye-sensitized solar cells (DSSCs) through rapid library synthesis by a one-pot procedure, Chem. Eur. J., 20 (2014) 10685-10694.
[16] Matsumura, K.; Yoshizaki, S.; Maitani, M. M.; Wada, Y.; Ogomi, Y.; Hayase, S.; Kaiho, T.; Fuse, S.; Tanaka, H., Takahashi, T. Rapid synthesis of thiophene-based, organic dyes for dye-sensitized solar cells (DSSCs) by a one-pot, four-component coupling approach, Chem. Eur. J., 21 (2015) 9742-9747.
[17] Fuse, S.; Takahashi, R.; Maitani, M. M.; Wada, Y.; Kaiho, T.; Tanaka, H., Takahashi, T. Synthesis and evaluation of thiophene-based organic dyes containing a rigid and nonplanar donor with secondary electron donors for use in dye-sensitized solar cells, Eur. J. Org. Chem., (2016) 508-517.
[18] Irie, S.; Fuse, S.; Maitani, M. M.; Wada, Y.; Ogomi, Y.; Hayase, S.; Kaiho, T.; Masui, H.; Tanaka, H., Takahashi, T. Rapid synthesis of D-A'-π-A dyes through a one-pot three-component Suzuki-Miyaura coupling and an evaluation of their photovoltaic properties for use in dye-sensitized solar cells, Chem. Eur. J., 22 (2016) 2507-2514.
[19] Fuse, S.; Takizawa, M.; Matsumura, K.; Sato, S.; Okazaki, S., Nakamura, H. Thiophene-based organic D-π-A dyes as potent sensitizers for photodynamic therapy, Eur. J. Org. Chem., (2017) 5170-5177.
[20] Fuse, S.; Matsumura, K.; Takizawa, M.; Sato, S., Nakamura, H. The design, synthesis, and evaluation of organic dithienopyrrole-based D-π-A dyes for use as sensitizers in photodynamic therapy, Bioorg. Med. Chem. Lett., 28 (2018) 3099-3104.
[21] Fuse, S.; Takizawa, M.; Sato, S.; Okazaki, S., Nakamura, H. Elucidating the mode of action for thiophene-based organic D-π-A sensitizers for use in photodynamic therapy, Bioorg. Med. Chem., 27 (2019) 315-321.
[22] Acrylic acid is deprotonated to generate corresponding carboxylate under physiological conditions. We confirmed this by measuring photoabsorption spectra under different pH. For details, see ref. 19 and 21.
[23] Pereira, J. B.; Carvalho, E. F. A.; Faustino, M. A. F.; Fernandes, R.; Neves, M. G. P. M. S.; Cavaleiro, J. A. S.; Gomes, N. C. M.; Cunha, Â.; Almeida, A., Tomé, J. P. C. Phthalocyanine thio-pyridinium derivatives as antibacterial photosensitizers, Photochem. Photobiol., 88 (2012) 537-547.
[24] Hirakawa, K.; Fukunaga, N.; Nishimura, Y.; Arai, T., Okazaki, S. Photosensitized protein damage by dimethoxyphosphorus(V) tetraphenylporphyrin, Bioorg. Med. Chem. Lett., 23 (2013) 2704-2707.
[25] Hirakawa, K.; Umemoto, H.; Kikuchi, R.; Yamaguchi, H.; Nishimura, Y.; Arai, T.; Okazaki, S., Segawa, H. Determination of singlet oxygen and electron transfer mediated mechanisms of photosensitized protein damage by phosphorus(V)porphyrins, Chem. Res. Toxicol., 28 (2015) 262-267.
[26] Hirakawa, K., Yoshioka, T. Photoexcited riboflavin induces oxidative damage to human serum albumin, Chem. Phys. Lett., 634 (2015) 221-224.
[27] Ouyang, D., Hirakawa, K. Photosensitized oxidative damage of human serum albumin by water-soluble dichlorophosphorus(V) tetraphenylporphyrin, Rapid Commun. Photosci., 4 (2016) 41-44.
[28] Ouyang, D.; Inoue, S.; Okazaki, S., Hirakawa, K. Tetrakis(*N*-methyl-*p*-pyridinio)porphyrin and its zinc complex can photosensitize damage of human serum albumin through electron transfer and singlet oxygen generation, J. Porphyrins Phthalocyanines, 20 (2016) 813-821.
[29] Fanali, G.; di Masi, A.; Trezza, V.; Marino, M.; Fasano, M., Ascenzi, P. Human serum albumin: from bench to bedside, Mol. Aspects Med., 33 (2012) 209-290.
[30] Mayor, S.; Parton, R. G., Donaldson, J. G. Clathrin-independent pathways of endocytosis, Cold Spring Harb. Perspect. Biol., 6 (2014) a016758.
[31] Kaksonen, M., Roux, A. Mechanisms of clathrin-mediated endocytosis, Nat. Rev. Mol. Cell Biol., 19 (2018) 313.
[32] Dutta, D., Donaldson, J. G. Search for inhibitors of endocytosis: Intended specificity and unintended consequences, Cell. Logist., 2 (2012) 203-208.
[33] Jones, A. T., Clague, M. J. Phosphatidylinositol 3-kinase activity is required for early endosome fusion, Biochem. J., 311 ( Pt 1) (1995) 31-34.
[34] Castano, A. P.; Demidova, T. N., Hamblin, M. R. Mechanisms in photodynamic therapy: part one—photosensitizers, photochemistry and cellular localization, Photodiagnosis Photodyn. Ther., 1 (2004) 279-293.